Modeling and Simulation of Rigid-Soft Hybrid HASEL-Actuated Robotic Swimmers

Mike Y. Michelis, Stephan-Daniel Gravert, Robert K. Katzschmann

***Abstract*—Little work exists on the modeling of electrostatically-actuated robotic systems, which severely hinder their application in controls or optimization in the real world. On the one hand, it is a rather new field of actuator technology, on the other hand, many simplifications need to be made to allow the model to be practically viable. We present several approaches to modeling soft robotic swimmers, in particular Peano-HASEL-actuated robots, where deformation of solids play a crucial role in generating the thrust forces in the fluid surrounding the robot. We will show how to model and simulate the electrostatic actuation of such swimmers, both in 2D and 3D, and apply them within fluid-structure interaction environments. We use simplified muscles in 2D to approximate the HASELs, while in 3D we use symbolic regression to find a relation between force and strain, which is then applied as loads on the HASEL attachment locations. These modeling techniques will sketch out several feasible approaches that can be used in downstream tasks such as control and shape optimization for these robotic systems equipped with electrostatic actuation.**

I. Introduction

Hydraulically Amplified Self-healing ELectrostatic (HASEL) actuators [1] have become a popular choice for bio-inspired muscles of soft robots [2], [3], yet the modeling often requires great simplification and more complex simulated systems have not yet been explored [4], [5]. Especially for simulations in real-world environments, such as underwater robots for exploration [6]–[9], proper modeling and simulation of HASELs is necessary. We explore several designs of electrostatically actuated swimmers, in 2D and 3D, with an according 2.5D fabricated swimmer that we use for simulation to reality matching. We use a variant of the HASEL called Peano-HASEL [10], [11] for the robotic swimmer, due to its biomimetic, contractile muscle-like behavior. We model the 2D robots in a differentiable simulation framework, DiffPD [12], with the future goal of optimizing its controls and topology. Since the framework does not yet support Fluid-Structure-Interaction (FSI), we model the 3D design in the commercial Finite Element Method (FEM) software COMSOL [13]. We show different methods of modeling the HASEL actuation forces, and apply them in a final 3D FSI setting with a thin swimmer tail flapping while submerged in fluid.

Authors are with the Soft Robotics Lab, Department of Mechanical and Process Engineering, ETH Zurich, 8092 Zurich, Switzerland michelism@ethz.ch

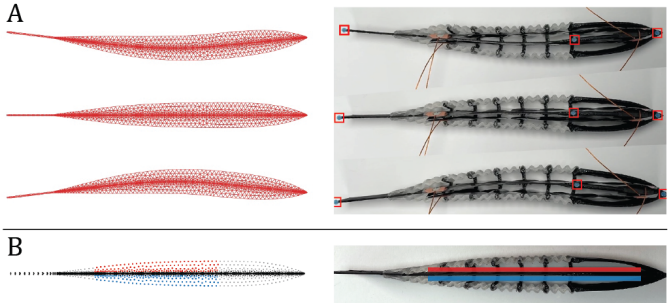

Fig. 1. Modeling of soft swimmer equipped with HASEL actuators using simplified model: external thin-wall structure and middle spine structure simplified, and density approximated. (A) shows a qualitative matching between simulated and real swimmers in bending angles, where the blue tracker markers are highlighted with red boxes, and (B) shows the location of the actuated muscles in simulation (left) and reality (right).

II. Method

A. 2.5D Simplified Swimmer

Following previous work on modeling soft robotic actuators using simplified muscles [12], [14]–[16], we first present our previous simplified, but efficient, approach [16] on simulating HASELs in Figure 1. We start with a simple 2D swimmer design with contractile muscles on either side, where the real-world equivalent is extruded in z-axis with constant height profile. This structure is printed on a multimaterial printer, with rigid polypropylene (PP) material and soft styrene-ethylene-butylene-styrene (SEBS) material, and is actuated using electrostatic HASEL muscles. Due to the antagonistic nature of the 2D swimmer muscles, we model triangular elements on both sides of the spine as muscle elements in the differentiable soft body simulation framework DiffPD [12]. These elements can expand and contract based on a scalar factor a, which will be our actuation input. The reason for the rigid middle spine is that in practical experiments we observe how this rigid structure improves forward thrust of the swimmer. Since the contraction factor a is no longer a physical value (such as voltage input on the HASEL), we are required to perform a sim-to-real matching for realistic muscle actuation behavior. This is quite easily achievable since the swimmer is modeled in a differentiable framework w.r.t. the muscle actuation, hence we can match the bending angle of the swimmer between simulation and reality by tracking motion markers on the real swimmer.

For collecting real-world data, we put three blue dot markers on the swimmer, at the head, middle, and tail of the robot

(red markers seen in Figure 1). These are tracked using the CSRT algorithm [17] throughout the motion of the swimmer, and we obtain a bending angle between the head-to-mid $\vec{v}_{HM}$ and mid-to-tail $\vec{v}_{MT}$ vectors, which will be independent of the global motion of the fish, i.e. even if the swimmer shifts around on the table our bending angles will capture the correct deformation. The sine of the bending angle θ is then computed as $\vec{v}_{MT}$ with $\sin\theta = (\vec{v}_{HM} \times \vec{v}_{MT})/(\|\vec{v}_{HM}\| \, \|\vec{v}_{MT}\|)$. We compute this bending angle both in simulation and reality, and optimize the muscle actuation a by minimizing the discrepancy $\mathcal{L}_a = \frac{1}{N}\sum_{i=1}^{N} \|\theta_{sim}(i) - \theta_{real}(i)\|^2$. The result of the optimized deformation can be seen in Figure 2. Next, we extend our previous work [16] with an accurate 2D geometry and a 3D model for FSI.

B. 2.5D Geometrically-Accurate Swimmer

Since the previous simplified muscles assumed a fully solid body as opposed to the hollow real-world fabricated swimmer, we had to set material parameters that were unrealistic, namely a soft material of $65\,\mathrm{kPa}$ and a rigid one of $0.13\,\mathrm{MPa}$. The realistic values are $0.65\,\mathrm{MPa}$ and $1.33\,\mathrm{GPa}$, respectively. We approximate the density with $900\,\mathrm{kg\,m^{-3}}$, and assume a Poisson's ratio of 0.45. As both the geometry and material parameters were estimated in the previous case, we wish to model the swimmer more accurately. To this end, we stay with the previous 2D model, but have more accurate geometry and more physical material parameters for the rigid and soft structures. This more accurate swimmer can be seen in Figure 3.

Because our thin-walled geometry matches now, we can try to use the material parameters given by the manufacturer. We use Young's moduli of $0.65\,\mathrm{MPa}$ and $0.13\,\mathrm{GPa}$ for soft and rigid material respectively. The rigid material is still 10 times softer, but after a lot of parameter tuning, the only method we could manage to have the soft body simulation converge was through a timestep of $dt = 0.01\,\mathrm{ms}$ instead of $dt = 0.01\,\mathrm{s}$. This would absolutely not make this method

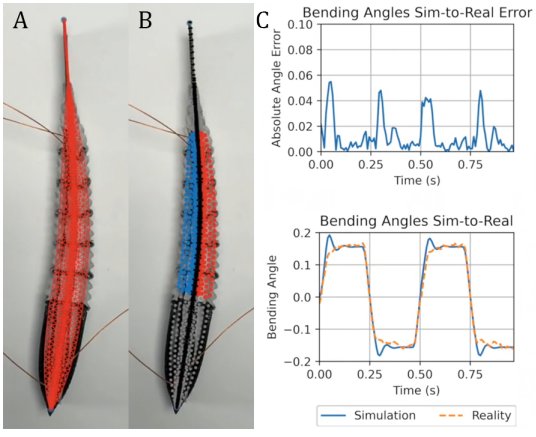

Fig. 2. Simulation to reality matching of simplified 2.5D swimmer. (A) shows the overlay of the simulated mesh over the real swimmer, while (B) shows the overlay of the element types over real swimmer. A quantitative comparison between simulation and reality is shown in (C).

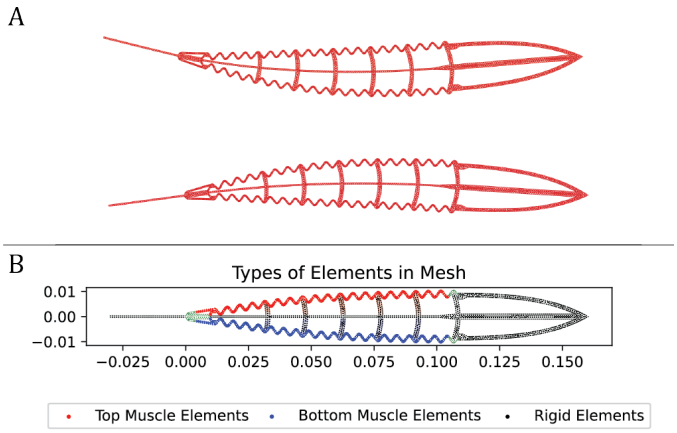

Fig. 3. Accurate geometric modeling of the 2.5D electrostatically-actuated swimmer, where the muscles are located in the outer shell of the swimmer. (A) displays the deformed meshes of the swimmer, and (B) shows the element types in the mesh, which ones are muscle, and which ones are rigid material.

usable in practice, hence we decided to soften the rigid material slightly for feasibility. As for the complexity of the accurate mesh compared to the simplified one, we have 1556 vertices in the more complex mesh, and 557 vertices for the simplified one. Runtimes on average were $853\,\mathrm{ms}$ and $482\,\mathrm{ms}$ respectively.

The main limitation with this approach, is how the muscle actuation is modeled. Since we can no longer define cells aside from the spine to be contractile muscles, we now define the outer walls of the swimmer to contract. This behavior can match the deformation of the corresponding real robot as well, however, an improved actuation model would be desired.

C. Electrostatic Actuation Modeling

These previous models have been matching the electrostatic actuation with simplified muscle actuators in simulation through real observed bending angles. No assumptions were made on the dynamical model of the electrostatic actuation in simulation. As a next step, we want to use experimental data from the HASEL actuators to define their actuation force in simulation. As observed in the fabricated swimmer, the HASELs are attached at the head and tail of the spine, where a force is contracting the spine on one side causing a bending behavior of the whole structure. We model this external force in simulation as point forces applied at the HASEL attachment points. Note that while contracting on one side, the opposite HASEL will be stretched, causing a counteracting force. This phenomenon we do not model currently, and will be important to match the realistic behavior accurately. For now we can neglect this effect due to the real HASELs not being fully stretched in neutral position, and even during actuation, they do not seem to be causing much counteracting forces.

As for the modeling of the HASEL forces, we base ourselves off of the analytical formula derived for Peano-HASELs [4]. They present a parametrized formulation with parameter

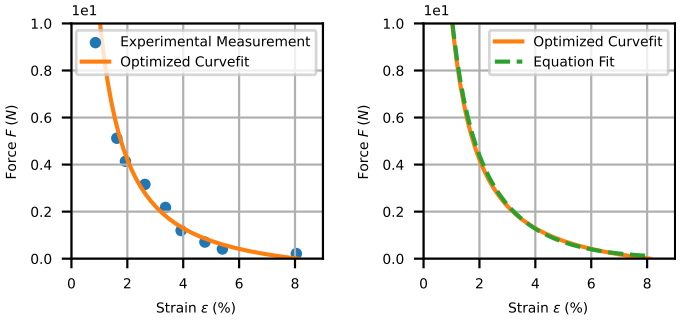

Fig. 4. Fitting parametric curve to experimental HASEL actuation data on the left, while the right plot shows the symbolic regression result and the equation that fits the experimentally fitted curve.

α for the force-strain relationship in the following form:

$$F = \frac{\cos(\alpha)}{1-\cos(\alpha)} a_1 \tag{1}$$

$$\varepsilon = 1 - a_2 \left(1 + a_3 \frac{\sin(\alpha) - \alpha}{\sqrt{\alpha - \sin\alpha\cos\alpha}}\right) \tag{2}$$

Here we merged all physical parameters into the constants a_i (including a fixed actuation voltage for the HASELs). The reason we do this, is such that we can gather experimental data and perform an optimization for these constants that best fit the observations. This is equivalent to doing a system identification on the physical parameters. In Figure 4 (left) the results can be seen of the curve defined by the optimized parameters a_i.

In order to apply external forces on our simulated swimmer constructs, we require a relation between the strain and force of the actuator directly. We use the equation discovery/symbolic regression framework PySR [18] to find a relation $F(\varepsilon)$. The relation we found most appropriate, which is also shown in Figure 4 (right), was:

$$F(\varepsilon) = \varepsilon + 21.71\left(\frac{1}{\varepsilon + 0.22} - 0.39\right) \tag{3}$$

In the next step we apply this fitted force directly onto a 3D model of an electrostatically actuated swimmer.

D. 3D HASEL Swimmer

We created a 3D model based on the previous design and typical biological fish shape references: a thin soft fin made from Polylactic Acid (PLA) that is actuated by Peano-HASELs which can be seen in Figure 5. We apply the previously computed forces on the two HASEL-attachment pins as can be seen in Figure 5A. The force is dependent on the distance between the pins, from which we compute the strain on the HASELs. Since our previous differentiable framework does not support FSI, we chose to model this 3D swimmer in COMSOL [13]. All material parameters were set to their physically correct values, except for the fluid density. The solver did not converge with a fluid density of $1000\,\mathrm{kg\,m^{-3}}$, it did with $100\,\mathrm{kg\,m^{-3}}$, hence for now we keep this model purely in simulation. The FSI fluid velocity field in Figure 5C should therefore be interpreted qualitatively, and not realistically. For the fluid simulation, we additionally attach a head that is fixed in space. This setup will in future work be used to compute forward thrust of such a swimmer design.

One parameter we had to tune, was the damping of the fin. We chose a Rayleigh damping with $\alpha = 10\,\mathrm{s}^{-1}$ and $\beta = 0.01\,\mathrm{s}$ such that no major oscillations occurred when maximal deformation is reached. This would be a parameter that should be experimentally tuned.

III. Discussion

Modeling HASEL-driven robots using simplified muscles provide a computationally efficient alternative, though sacrificing generalizability since the simplified muscles are often calibrated to match experimental data. We observed that the increase in geometric complexity was not the main bottleneck, but rather the material stiffness of the more rigid spine material in the 2.5D swimmer.

The 3D FEM simulation suffers from an empirical estimate of the damping parameters, which should be improved in the future with more precise experimental estimates. A big limitation of our 3D model of the swimmer, is that the Peano-HASELs are not assumed to have any mechanical impedance, i.e. we assume they can be stretched without any resistance. In practice, the HASELs are rarely stretched to perfect tension, hence they will not be stretched enough to cause resistance. But this should be taken into account in future models, and can be easily added using a counteracting force. Similar to how we measure the force-strain curve for actuated HASELs, we can build a force-strain curve for unactuated HASELs, and see what resisting forces exist when external weights are stretching the HASEL. This can be incorporated in the robotic system where the HASEL resistance to stretching is given by this unactuated force-strain curve.

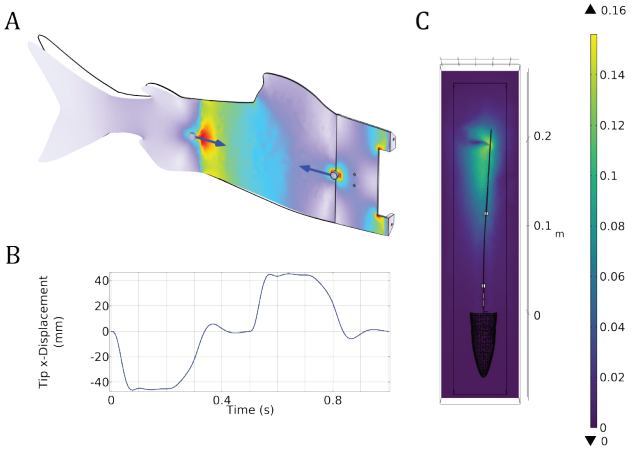

Fig. 5. COMSOL simulation of 3D swimmer actuated by HASELs for left-right flapping motion. (A) Blue arrows indicate HASEL forces that cause contraction. (B) shows the deformation outside of fluid, while (C) displays the FSI velocity magnitude of the fluid.

Another limitation is how the force should be velocity-dependent in practice. Currently we assume that forces are given at certain strains, and simply apply that force to the pins where the HASELs attach to the robot. The force-strain curve is measured as the blocking force, i.e. when the HASEL is static and not moving. In reality, it is likely that more force is generated at lower actuation velocities. This points towards our current force estimates being too high, and deformation being larger than expected in reality.

Lastly, the 3D model is a purely simulated model, since we did not have realistic fluid parameters yet. As a next step we would like to incorporate our swimmer design into a fluid with equivalent parameters to water (10 time heavier density).

IV. Conclusion and Future Works

In this work, we presented 2D and 3D models for HASEL-actuated robotic swimmers. We show how electrostatic actuation can be modeled using simplified muscles and through symbolic regression based on experimental data. Lastly we show the actuation of the swimmer in a 3D FSI environment, showing how it qualitatively generates the vortices that create forward thrust.

In the future we wish to bring these simulated robots into the real world, while optimizing their geometrical shape and actuation signal either using gradient-based optimization in combination with differentiable simulations, or using gradient-free parameter searches in commercially available frameworks such as COMSOL. This will open up the possibility of bringing soft, actuated robots into real-world environments, such as underwater exploration, without loud, heavy machinery polluting our lakes, rivers, and oceans.

References

[1] P. Rothemund, N. Kellaris, S. K. Mitchell, E. Acome, and C. Keplinger, "Hasel artificial muscles for a new generation of lifelike robots—recent progress and future opportunities," *Advanced Materials*, vol. 33, no. 19, p. 2003375, 2021. [Online]. Available: https://onlinelibrary.wiley.com/doi/abs/10.1002/adma.202003375

[2] N. Kellaris, P. Rothemund, Y. Zeng, S. K. Mitchell, G. M. Smith, K. Jayaram, and C. Keplinger, "Spider-inspired electrohydraulic actuators for fast, soft-actuated joints," *Advanced Science*, vol. 8, no. 14, p. 2100916, 2021.

[3] P. Rothemund, N. Kellaris, S. K. Mitchell, E. Acome, and C. Keplinger, "Hasel artificial muscles for a new generation of lifelike robots—recent progress and future opportunities," *Advanced Materials*, vol. 33, no. 19, p. 2003375, 2021.

[4] N. Kellaris, V. G. Venkata, P. Rothemund, and C. Keplinger, "An analytical model for the design of peano-hasel actuators with drastically improved performance," *Extreme Mechanics Letters*, vol. 29, p. 100449, 2019.

[5] Y. Yeh, N. Cisneros, Y. Wu, K. Rabenorosoa, and Y. Le Gorrec, "Modeling and position control of the hasel actuator via port-hamiltonian approach," *IEEE Robotics and Automation Letters*, 2022.

[6] A. D. Marchese, C. D. Onal, and D. Rus, "Autonomous soft robotic fish capable of escape maneuvers using fluidic elastomer actuators," *Soft Robotics*, vol. 1, no. 1, pp. 75–87, 2014, pMID: 27625912. [Online]. Available: https://doi.org/10.1089/soro.2013.0009

[7] R. K. Katzschmann, J. DelPreto, R. MacCurdy, and D. Rus, "Exploration of underwater life with an acoustically controlled soft robotic fish," *Science Robotics*, vol. 3, no. 16, p. 3449, 3 2018. [Online]. Available: http://robotics.sciencemag.org/

[8] J. Shintake, V. Cacucciolo, H. Shea, and D. Floreano, "Soft biomimetic fish robot made of dielectric elastomer actuators," *Soft Robotics*, vol. 5, no. 4, pp. 466–474, 2018, pMID: 29957131. [Online]. Available: https://doi.org/10.1089/soro.2017.0062

[9] W. Tang, Y. Lin, C. Zhang, Y. Liang, J. Wang, W. Wang, C. Ji, M. Zhou, H. Yang, and J. Zou, "Self-contained soft electrofluidic actuators," *Science Advances*, vol. 7, no. 34, p. eabf8080, 2021. [Online]. Available: https://www.science.org/doi/abs/10.1126/sciadv.abf8080

[10] N. Kellaris, V. Gopaluni Venkata, G. M. Smith, S. K. Mitchell, and C. Keplinger, "Peano-hasel actuators: Muscle-mimetic, electrohydraulic transducers that linearly contract on activation," *Science Robotics*, vol. 3, no. 14, p. eaar3276, 2018.

[11] S. K. Mitchell, X. Wang, E. Acome, T. Martin, K. Ly, N. Kellaris, V. G. Venkata, and C. Keplinger, "An easy-to-implement toolkit to create versatile and high-performance hasel actuators for untethered soft robots," *Advanced Science*, vol. 6, no. 14, p. 1900178, 2019. [Online]. Available: https://onlinelibrary.wiley.com/doi/abs/10.1002/advs.201900178

[12] T. Du, K. Wu, P. Ma, S. Wah, A. Spielberg, D. Rus, and W. Matusik, "Diffpd: Differentiable projective dynamics," *ACM Transactions on Graphics*, vol. 41, no. 2, nov 2021.

[13] C. Multiphysics, "Introduction to comsol multiphysics®," *COMSOL Multiphysics, Burlington, MA, accessed Feb*, vol. 9, p. 2018, 1998.

[14] S. Min, J. Won, S. Lee, J. Park, and J. Lee, "Softcon: Simulation and control of soft-bodied animals with biomimetic actuators," *ACM Transactions on Graphics (TOG)*, vol. 38, no. 6, pp. 1–12, 2019.

[15] M. Dubied, M. Y. Michelis, A. Spielberg, and R. K. Katzschmann, "Sim-to-real for soft robots using differentiable fem: Recipes for meshing, damping, and actuation," *IEEE Robotics and Automation Letters*, vol. 7, no. 2, pp. 5015–5022, 2022.

[16] S.-D. Gravert, M. Y. Michelis, S. Rogler, D. Tscholl, T. Buchner, and R. K. Katzschmann, "Planar modeling and sim-to-real of a tethered multimaterial soft swimmer driven by peano-hasels," *arXiv preprint arXiv:2208.00731*, 2022.

[17] A. Lukezic, T. Vojir, L. ˇCehovin Zajc, J. Matas, and M. Kristan, "Discriminative correlation filter with channel and spatial reliability," in *Proceedings of the IEEE conference on computer vision and pattern recognition*, 2017, pp. 6309–6318.

[18] M. Cranmer, A. Sanchez-Gonzalez, P. Battaglia, R. Xu, K. Cranmer, D. Spergel, and S. Ho, "Discovering symbolic models from deep learning with inductive biases," *NeurIPS 2020*, 2020.